Appl. Phys. A 75, 79–88 (2002) / Digital Object Identifier (DOI) 10.1007/s003390101057

Applied Physics A
Materials
Science & Processing

First-principles studies of kinetics in epitaxial growth of III–V semiconductors

P. Kratzer*, E. Penev, M. Scheffler

Fritz-Haber-Institut der Max-Planck-Gesellschaft, Faradayweg 4–6, 14195 Berlin, Germany

Received: 2 May 2001/Accepted: 23 July 2001/Published online: 3 April 2002 –

Abstract. We demonstrate how first-principles calculations using density-functional theory (DFT) can be applied to gain insight into the molecular processes that rule the physics of materials processing. Specifically, we study the molecular beam epitaxy (MBE) of arsenic compound semiconductors. For homoepitaxy of GaAs on GaAs (001), a growth model is presented that builds on results of DFT calculations for molecular processes on the β2-reconstructed GaAs (001) surface, including adsorption, desorption, surface diffusion, and nucleation. Kinetic Monte Carlo simulations on the basis of the calculated energetics enable us to model MBE growth of GaAs from beams of Ga and As_2 in atomistic detail. The simulations show that island nucleation is controlled by the reaction of As_2 molecules with Ga adatoms on the surface. The analysis reveals that the scaling laws of standard nucleation theory for the island density as a function of growth temperature are not applicable to GaAs epitaxy. We also discuss heteroepitaxy of InAs on GaAs (001), and report first-principles DFT calculations for In diffusion on the strained GaAs substrate. In particular, we address the effect of heteroepitaxial strain on the growth kinetics of coherently strained InAs islands. The strain field around an island is found to cause a slowing down of material transport from the substrate towards the island, and thus helps to achieve more homogeneous island sizes.

PACS: 68.55.Ac; 68.35.Fx; 71.15.Nc

In the last decade, research in semiconductor heterostructures has evolved into one of the most active fields in semiconductor physics. Progress in this field owes much to advanced growth methods such as molecular beam epitaxy (MBE) and metal-organic vapor-phase epitaxy (MOVPE). Using these techniques, heterostructures from compound semiconductor materials can be grown with high precision. The quantum-well and quantum-dot structures obtained in this way are of considerable technological interest, since they are used as active components in devices, e.g. in high-electron-mobility transistors and optoelectronics. The possibility to design well-defined nanostructures or nanostructured materials by epitaxial growth techniques has raised the desire to understand and eventually control growth on the atomic scale. While important input to such an understanding comes from probes with atomic resolution, in particular from scanning tunneling microscopy (STM) studies, theoretical input from growth simulations is equally important. Only a combined approach, using the results of modeling to interpret experimental data, will enable us to bring to light all the atomistic details involved in the fairly complex growth process of a compound semiconductor material.

At the atomic level, understanding MBE and MOVPE requires knowledge about the chemical reactions between the substrate surface and the atoms or molecules used as reactants (frequently called 'precursors' in the MOVPE literature), in addition to knowledge about the processes occurring on the surface, such as diffusion, nucleation, and attachment or detachment of adatoms to existing islands and steps. In recent years, there has been considerable progress in the understanding of surface chemical reactions using ab initio methods. In particular, total-energy calculations on the basis of density-functional theory (DFT) have proven to be most helpful for describing reactions in a fairly complex atomic environment, e.g. at a reconstructed surface. The dynamics of individual reactive encounters with a surface have been modeled in great detail; either by integrating the classical trajectory of a molecule over a few hundred femtoseconds, or by the use of quantum-mechanical scattering techniques [1, 2]. In contrast to elementary reactions, when modeling epitaxial growth, the properties of interest (e.g. the growth morphology) develop only over time scales of the order of seconds and length scales of micrometers, while the ruling microscopic processes operate in the length and time domains of 0.1–1 nm and femto- to picoseconds. Hence, the use of DFT calculations for modeling atomistic aspects of growth has been hampered by the need to bridge length and time scales by many orders of magnitude. First-principles molecular dynamics studies, while being very useful in the investigation of individual events on time scales shorter than 100 ps, are not suitable for access-

*Corresponding author.
(Fax: +49-30/8413-4701, E-mail: kratzer@fhi-berlin.mpg.de)

ing the time scales involved in growth, nor can they tackle the statistical interplay of the numerous processes that are responsible for the outcome of a growth experiment. As will be shown in this paper, kinetic Monte Carlo (kMC) simulations offer an efficient and accurate way to cope with this difficulty.

The relevance of physical chemistry for the elementary steps in compound semiconductor epitaxy was realized more than twenty years ago [3]. While deposition of elemental metal films involves the diffusion and nucleation of a single species, MBE and, to an even larger extent, MOVPE, involves reactions of molecular species, either among each other or with the surface. Any of these elementary steps could in principle be rate-limiting, or affect in some way the growth morphology. Principal considerations of this kind, exemplified by kinetic Monte Carlo studies, led Ghaisas and Madhukar to the distinction between diffusion-limited and reaction-limited growth [4, 5] in the context of GaAs epitaxy.

However, most of the work in the last decade has put aside the additional complexity introduced by surface reactions. A single 'effective' species, usually assumed to be gallium, moving on a simple cubic lattice [6, 7], or sometimes on the more physical face-centered cubic lattice [8], was employed for modeling of GaAs epitaxy. Mainly motivated by the different time scales involved in the oscillations of the RHEED (reflection high energy electron diffraction) signal and in its recovery after a growth interruption, a model with two species, Ga atoms and GaAs molecules, was introduced [9–11]. Recently, Ishii and Kawamura also treated a two-component model with both Ga and As atomic species [12, 13]. Both these two-component models restricted themselves to a simple cubic lattice. The aspect of surface reconstruction was not addressed until recently when Itoh et al. [14] presented results of a more refined modeling including the interactions between surface As dimers, as well as the anisotropy of Ga diffusion on the reconstructed GaAs surface.

By adopting suitable model parameters guided by experimental input from a detailed STM study, Itoh et al. were able to simulate the morphology, the size, and the density of small islands in very good agreement with the experimental observations [15, 16]. Yet the 'reconstruction' of a growth model on an empirical basis, working backwards from the analysis of experimentally observed growth features, is a tedious and, given the complexity of the problem, sometimes ambiguous procedure. Without knowledge of the most likely microscopic processes, it is difficult to decide which of two alternative elementary steps should be part of the growth model when both give rise to similar growth features. It appears much more appealing to construct a growth model in a 'bottom-up' fashion, starting from knowledge about the atomic processes obtained from first-principles total-energy calculations. As an additional benefit from such an approach, we obtain an immediate identification between the processes included in the model and the motion of atoms involved in growth. This is in contrast to empirical growth models, where 'effective' processes are used to rationalize experimental findings, but difficulties may arise later when attributing these 'effective' processes to real physical processes.

In the epitaxy of metals, there has been considerable progress in recent years triggered by a microscopic understanding of growth on the basis of density-functional total-energy calculations [17–20]. Although the homoepitaxy of a metal on a close-packed surface appears at first to be a fairly simple problem, detailed experiments in conjunction with kinetic simulations on the basis of first-principles results have revealed a number of fascinating details. Despite the obvious fact that epitaxy of compound semiconductors is an even more complex problem, due both to their two-component nature and the complexity of their surface structure, we feel encouraged by the progress due to the use of first-principles methods achieved for metallic systems, and were tempted to extend this approach to molecular beam epitaxy of compound semiconductors.

1 Homoepitaxy of GaAs

1.1 Present understanding

In this section, we shall describe a model for MBE homoepitaxy of GaAs on a GaAs (001) substrate from Ga atoms and As_2 molecules that has been constructed on the basis of density-functional total-energy calculations. We are aiming at a simulation of the atomistic processes of island growth including all relevant microscopic details, such as the surface reconstruction, different kinetic properties of the species involved, etc., based on the understanding we obtain from first-principles calculations of the energetics. Specifically, we model island growth on the well-known (2×4) reconstructions of GaAs (001) that prevail under frequently used growth conditions. Several theoretical investigations [21–26] have contributed to our present understanding of the atomic structure of this surface. The starting point for our modeling is the $\beta 2\,(2 \times 4)$ reconstruction of GaAs (001). This moderately As-rich surface reconstruction is terminated by pairs of As dimers, which alternate with 'trenches' running in the $[\bar{1}10]$ direction (missing a pair of As dimers and two Ga atoms per unit cell in the two topmost layers). Recently, a combined theoretical and experimental STM study has unequivocally shown that this reconstruction is the ground state of the surface when carefully prepared at temperatures around 550 °C and conditions typical for MBE [27]. Other (2×4) reconstructions that are energetically close to $\beta 2$ (see [25] and references given therein) and could possibly show up on the surface during growth are the α and $\beta 1$ (also just called β) reconstructions. They evolve out of the $\beta 2$ structure by adding two Ga atoms in the trench (α) and by further adding two As atoms, forming a third As dimer in the top layer ($\beta 1$). Recently, it has also been discussed whether the $\alpha 2$ structure, which results from the $\beta 2$ structure by desorbing one of the top-layer As dimers, could be observed under particular conditions [26, 28, 29]. Only when growth conditions very different from the standard ones are employed can major changes of the surface reconstruction leading to different symmetries occur. At lower growth temperatures, as used e.g. for heteroepitaxy of InAs on GaAs [30], one typically has a more As-rich chemical environment in the growth chamber. This gives rise to a $c(4 \times 4)$ reconstruction of the GaAs (001) surface, where the two topmost layers consist entirely of As atoms [31]. In the other extreme, annealing of the GaAs (001) surface in vacuum results in the Ga-rich (4×2) surface [32, 33]. Homoepitaxy on these surfaces, as well as the phase transitions between structures of different symmetry, is beyond the scope of this paper.

Both experimental knowledge and previous theoretical studies agree that arsenic and gallium behave quite differently on the GaAs (001) (2×4) surface. While Ga atoms adsorb with unit sticking probability, As_2 molecules only stick to the surface after Ga has been deposited [3, 34]. These findings have been substantiated by recent calculations using density-functional theory [35, 36]. While Ga adatoms were found to bind strongly (between 1.5 and 2.1 eV at various surface sites) [37], the binding sites for As_2 molecules at a perfect GaAs (001)-β2 surface are either much weaker, or only accessible after traversing a considerable activation barrier [36, 38]. The rather weakly bound states of As_2 present on an ideal GaAs (001) surface are not sufficiently long-lived at standard growth temperatures to give rise to incorporation of molecules, but lead to temporary trapping of molecules close to the surface. However, as soon as Ga adatoms are present on the surface, stronger binding sites for the As_2 molecules arise that are accessible from the gas phase without a barrier [36].

On the Ga-precovered GaAs (001)-β2 surface, it is not compulsory for the As_2 to dissociate upon adsorption, because a gas-phase As_2 molecule can attach itself to the Ga adatoms and get incorporated by transforming itself into a surface As dimer. The growth model presented here is based on this low-energy pathway to arsenic incorporation. The weaker binding sites for As_2 on the pristine β2 surface are accounted for by introducing a short-lived molecular precursor state[1]. The As_2 molecules trapped in this state have the chance to explore an average number of surface sites, before they either desorb or find excess Ga to attach to. We account for this effect of the precursor in our model by working with an effective As_2 flux that is a factor of about 100 higher than the external flux from the As_2 source. The role of the As_2 precursor in growth is in accordance with previous experimental findings [3] as well as with computer simulations [14]. We also point out that the GaAs (001) surface, given that the β2 reconstruction with moderate additional Ga coverage persists during growth, offers only a very limited number of strong binding sites for As_2 molecules. For sufficient As incorporation to occur during growth, it is plausible that a mobile precursor state assists the As_2 molecules in finding the suitable sites with excess Ga needed for their adsorption. In accordance with previous investigations [14], we further assume that the mobility of arsenic on the surface is mainly not due to diffusion of As adatoms, but originates from As_2 in the mobile molecular precursor state. In fact, single As adatoms are not included in the present modeling, because their formation would require breaking of the strong As–As molecular bond (4 eV), and hence is an unlikely event.

For the Ga species, on the other hand, the mobility is completely determined by surface diffusion. Hence, a detailed account of Ga diffusion is a prerequisite for modeling the morphology of the growing surface. Ga mobility is essential for growth because sites for strong As_2 chemisorption are created only after a suitable local arrangement of Ga adatoms. In the context of DFT calculations, the potential-energy surface (PES) of an adatom is the adequate concept to address the issue of diffusion. DFT calculations of potential-energy surfaces for various GaAs (001) surfaces are available from the literature, both for Ga diffusion [39–41] as well as for As diffusion [42]. Most importantly, it was found (see [40]) that Ga has its strongest adsorption site inside As surface dimers, thereby breaking the dimer bond. The picture evolving from these computational results suggests that a possible role of the Ga atoms in growth could be the breaking up of existing As surface dimers, and the formation of locally Ga-rich environments that act as selective sites for adsorption of As_2 molecules from the gas phase.

In Sect. 1.2, we investigate the consequences of the energetics, as obtained from DFT calculations, for the statistical interplay of the various surface species during growth. In particular, we are interested in the statistics of island nucleation and its dependence on the growth conditions. To this end, we have performed kinetic Monte Carlo simulations for an atomistic growth model that includes the most relevant microscopic details.

1.2 Kinetic Monte Carlo simulations

In order to simulate epitaxial growth, we employ a mathematical model of the crystal, describing it as a three-dimensional lattice with the zincblende crystal structure. Ga and As atoms are occupying different sublattices. It is required that the position of each atom in the simulation can be associated with a lattice site. The crystallographic directions [110], [$\bar{1}$10], and [001] define the x, y, and z axes of the coordinate system. The crystal grows in the z direction. With each lattice site we associate a discrete variable describing the state of this site. In the present case, a site can be either empty or occupied by a Ga or an As atom. This discrete variable also carries the information about the local bonding of surface atoms different from those of bulk atoms due to surface reconstructions. Arsenic atoms in the topmost anion layer form As dimers, unless a Ga atom is sitting in them. The starting surface is prepared in the thermodynamic ground state, the β2 reconstruction of GaAs (001). Some randomly selected unit cells, however, are given in the β1 reconstruction, as this is energetically very close to the β2 reconstruction. The probability for a surface unit cell to be in the β1 structure when the simulation is started is determined from a Boltzmann distribution, where the calculated difference in surface energy per unit cell between the β1 and β2 reconstructions (360 meV [25]) is used in the exponent.

Time evolution proceeds by discontinuous changes of the occupation of discrete lattice sites. These events may be either adsorption or desorption of atoms or molecules, or the hopping of an atom from one site to another. Each event is characterized by a rate, which is determined prior to starting the simulation. We use a parameter-free approach to determine the rates on the basis of the energetics obtained from DFT calculations.

In the following we describe the events included in the present simulation in more detail.

– Ga adsorption
  Ga adsorption occurs with a probability given by the Ga flux times the area of the sample. A Ga flux of 0.1 ML/s typical for MBE growth is used in the simulations. A random site in the xy plane is selected for Ga adsorption; the layer where the adsorption takes place is determined by the local height of the surface. If this site is occupied or

[1] The term 'precursor' is used here in the sense as in surface science, meaning a weakly bound molecular state preceding the eventual transition to a chemisorbed (often dissociated) state.

unsuitable for adsorption, one of the four nearest-neighbor sites is selected. If all of these are occupied or unsuitable, the Ga atom is assumed to be reflected into the gas phase. Other Ga desorption events are not considered in the model.

– Ga surface diffusion
  Investigation of the Ga adatom diffusion starts with the calculation of the PES, which requires the determination of the optimum geometry and the total energy of the adatom and the substrate for a number of fixed lateral positions of the adatom. For each position, a DFT calculation including a structural optimization is performed. Special care must be taken of the fact that the PES may in general be a multi-valued function of the adatom position, in particular if the adsorbate can occupy substitutional or subsurface sites, or if it induces bond breaking in the substrate. For an example, we refer the reader to [40]. The energy minima in the PES obtained in this way are mapped onto sites of the lattice used for the kMC simulation. The rates for hops between two lattice sites are determined from the energy difference ΔE between the minimum corresponding to the initial position of the adatom and the relevant saddle point for hopping to a neighboring minimum. Using transition-state theory, it is also possible to determine the prefactors from first principles (see e.g. [43]). For Ga diffusion on GaAs (001), previous calculations have found prefactors of the order of 10^{12} to $10^{13}\ \mathrm{s}^{-1}$ for all hopping processes considered [40, 44]. Thus, the effect of possible prefactor variations is expected to be small. In the present work, we use a common prefactor of $10^{13}\ \mathrm{s}^{-1}$ for all processes. Due to the surface reconstruction, the rates for hopping of Ga adatoms are highly site-specific. We include 10 different hopping processes for an isolated Ga adatom in our model. For Ga atoms with one or two Ga next-nearest neighbors, different hopping rates modified by the binding energy between Ga atoms in these configurations are used [35]. In total, we differentiate between 29 hopping processes of Ga.
– Ga incorporation
  The DFT calculations show that binding of a Ga atom in some configurations is so strong that it is unlikely that the Ga atom will leave this site again during the time span of the simulation. Such an incorporation event takes place
  – if As is adsorbed above the Ga atom,
  – if it forms a dimer with a Ga neighbor in [110] direction in the top layer,
  – if it sits in the interior of a string of Ga atoms in $[\bar{1}10]$ direction.
– As_2 adsorption
  In the simulation, adsorption of As_2 can occur only at specific surface sites. At these sites, the adsorbing As_2 molecule becomes incorporated as an As surface dimer, with the dimer axis oriented along $[\bar{1}10]$. This is motivated by DFT calculations which show that the binding is sufficiently strong only if the As_2 forms three or four backbonds to the surface. Figure 1 illustrates two examples of sites where an As_2 molecule (shown in grey) has adsorbed. The As dimer has filled a pair of empty sites in the anion sublattice, surrounded by at least three (out of a possible four) Ga atoms on the cation sublattice. Upon adsorption, a dangling bond of each Ga atom is converted into an As–Ga bond. Possible As_2 adsorptions at other, weaker binding sites are considered as part of the As_2 precursor state, and are accounted for by a renormalized effective As_2 flux in our model. Since there are Ga atoms with dangling bonds in both sidewalls of the trench, a single additional Ga adatom in the trench is sufficient to form an arrangement with three Ga dangling bonds, and hence to create an adsorption site for As_2. This is in contrast to As_2 adsorption in the top layer, where at least three adatoms in adjacent sites are needed for that purpose. Thus As_2 adsorption in the trench is more likely to occur in the early stages of growth. However, adsorption of two adjacent As_2 molecules parallel to each other in the trench is disallowed in our model, unless at least one Ga atom has already adsorbed next to the trench. This is motivated by the results of a DFT calculation [35] showing that adsorption of a second As dimer next to an existing one in the trench (which would level out the trench) is unfavorable. Previous DFT calculations [45] demonstrated that the presence of Ga atoms in the neighborhood of the prospective adsorption site for As_2 significantly enhances the binding energy of the As_2 at this site. Therefore, adsorption of the last missing As dimer that levels out the trench is enabled in the simulations only after a Ga atom has adsorbed in its vicinity.

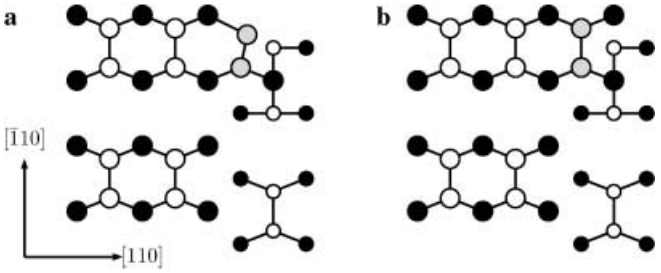

Fig. 1. a As_2 molecule (*grey*) adsorbed on a single Ga adatom that has split a trench As dimer, establishing three As–Ga backbonds, thereby forming a Ga–As–As–Ga_2 complex; **b** adsorbed on two Ga adatoms in the trench, establishing four As–Ga backbonds, thereby forming a Ga_2–As–As–Ga_2 complex. Arsenic atoms of the β2 reconstruction are shown as *empty circles*, gallium atoms as *filled circles*

– As_2 desorption
  Our model differentiates between three As_2 desorption events with different rates, depending on the chemical environment the As_2 is bonded to. These are
  – desorption of As_2 from sites where it had three backbonds to Ga atoms ($\Delta E = 1.9\,\mathrm{eV}$),
  – desorption of As_2 from sites where it had four backbonds to Ga atoms, but was misaligned with an adjacent As dimer row ($\Delta E = 1.9\,\mathrm{eV}$),
  – desorption of one of the outermost As_2 from a row of three adjacent As surface dimers (local β structure, $\Delta E = 2.4\,\mathrm{eV}$). In this case, the desorbing As dimer had four backbonds to Ga. Despite the high barrier for this process, it is necessary to include it to make it possible for the β1 structure to decay to the ground state of the surface, which is the β2 structure.

  In all cases an Arrhenius law for the desorption rate with a prefactor of $10^{13}\ \mathrm{s}^{-1}$ is used, following the analysis of experimental desorption data in the literature [46].

1.3 Results of the simulations

The simulations reveal that island growth is governed by the interplay of processes that occur on a hierarchy of time scales. In the following, we illustrate the situation for deposition at a surface temperature of 800 K. The shortest time scales (10^{-12}–10^{-9} s) are set by the hopping diffusion of Ga adatoms. Since hopping in the [$\bar{1}$10] direction along the trenches is faster than hopping from one trench to another in the [110] direction, Ga diffusion on the GaAs (001)-β2(2 × 4) surface is anisotropic. The terminating As dimers of the β2 reconstruction, in particular those in the trenches, can act as traps for diffusing Ga atoms, where they are immobilized for 10^{-8} s. At sites where a Ga atom has been adsorbed in a trench site, a gas-phase As_2 molecule can adsorb readily by establishing three bonds to surface Ga atoms, one of them to the Ga adatom and two other bonds with unsaturated Ga atoms that are already present in the β2 reconstruction in the slopes of the trenches. We refer to the structures resulting after As_2 adsorption as Ga–As–As–Ga_2 complexes (Fig. 1a). At temperatures below 800 K, such complexes have a mean lifetime of 0.1 s or more, long enough to react with another diffusing Ga adatom. This transforms them into even more long-lived Ga_2–As–As–Ga_2 complexes (Fig. 1b), that can be considered as unit cells in a local β1 reconstruction. The meta-stability of these intermediate structures is related to the local fulfillment of the electron-counting rule, i.e. no induced electronic states in the principal band gap are present after an atomic arrangement corresponding to local β1 reconstruction has been reached. We note that the importance of intermediate structures fulfilling the electron-counting rule was pointed out earlier [47, 48].

The role of the As_2–Ga complexes in growth becomes apparent from an analysis of the balance between adsorbing and desorbing As_2 fluxes during a kMC simulation. The speed of incorporation of arsenic into the substrate is given by the difference between the adsorbing flux and the desorbing flux F_{des}. In Fig. 2, we decompose the adsorbing flux into a contribution $F_{\mathrm{ads}}^{(3)}$ from Ga–As–As–Ga_2 and $F_{\mathrm{ads}}^{(4)}$ from Ga_2–As–As–Ga_2 complexes, respectively. These are compared to the net incorporated flux, $F_{\mathrm{As}} = F_{\mathrm{ads}}^{(3)} + F_{\mathrm{ads}}^{(4)} - F_{\mathrm{des}}$. We find that, at $T = 800$ K, the main route for chemisorption of incoming As_2 molecules is the formation of Ga–As–As–Ga_2 complexes. These are formed by As_2 reacting with single Ga adatoms at trench sites. The simultaneous reaction of As_2 with two adjacent Ga adatoms, leading to the Ga_2–As–As–Ga_2 complex, takes place as well, but contributes less to the net incorporation. The Ga–As–As–Ga_2 complexes must be considered as transient species that are only formed during growth. They either decay by desorption of As_2 or become stabilized by addition of another Ga adatom. In the latter case, we say that the chemisorbed As_2 has become incorporated into the surface, because it has achieved four backbonds to Ga, and desorption from this state is an infrequent event. Since this incorporated state is typically reached via the intermediate Ga–As–As–Ga_2 complex, the latter plays the role of a 'doorway' state for the incorporation of As_2.

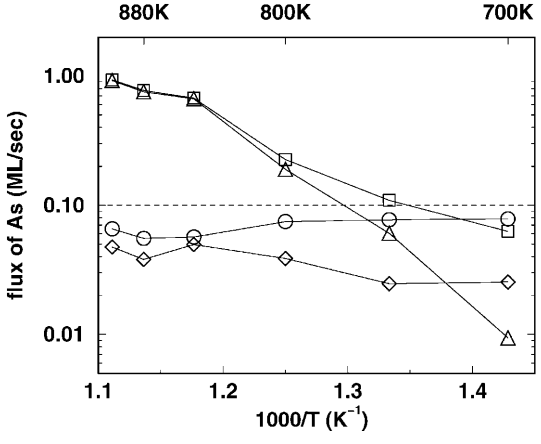

Fig. 2. Arsenic flux as a function of temperature during stationary island growth. Net As incorporation (*circles*) results from a balance between desorption (*triangles*) and adsorption forming three Ga–As backbonds (*squares*) or four Ga–As backbonds (*diamonds*). The maximum possible growth rate determined by the Ga flux is indicated by the *dashed horizontal line*

Further support for its importance for As_2 incorporation comes from the observation that the sticking probability of As_2 molecules for this pathway is first-order in the Ga coverage, because a single Ga atom in a trench site is sufficient to initiate the formation of the Ga–As–As–Ga_2 complex. This is in agreement with the experimentally observed reaction order [3]. Figure 2 shows that the net incorporation rate of arsenic decreases slightly at $T > 800$ K, and the adsorption due to Ga–As–As–Ga_2 complexes is almost completely consumed by a desorption flux of the same magnitude. At $T = 850$ K, the net arsenic incorporation is mainly due to direct reactive formation of the more strongly bound Ga_2–As–As–Ga_2 complexes. Eventually, at the highest temperatures, even these structures, forming part of groups of three As surface dimers (local β1 reconstruction), become unstable against desorption. At $T = 850$ K, the rate for this desorption process ($\Delta E = 2.4$ eV) is $0.06\,\mathrm{s}^{-1}$. This compares favorably with reported desorption processes associated with the formation of the β2 surface structure in this temperature range [49].

We note that the chemisorbed flux of arsenic, $F_{\mathrm{ads}}^{(3)} + F_{\mathrm{ads}}^{(4)}$, over the whole temperature range in Fig. 2 lies between 0.1 ML/s and 1 ML/s. For a Ga flux of 0.1 ML/s, this corresponds to a V/III ratio between 1 and 10, in agreement with frequently used experimental conditions for MBE growth. The much higher effective As_2 flux of 100 ML/s used in the simulation just reflects the average number of attempts that an As_2 molecule in the mobile precursor state makes to find a suitable site for chemisorption before it desorbs from the precursor. Taking the As flux that reaches the chemisorbed state as a measure, the impinging flux used in the simulation leads to values for arsenic chemisorption in the right order of magnitude.

For a further test of the growth model, we compare the island densities in the simulations with measured island densities. The comparison is made for the saturated island density reached after some fraction of a monolayer has been deposited. When this island density is reached, attachment of a deposited Ga atom to an existing island typically takes place before the adatom could take part in a new nucleation event. This leads to a very small rate of nucleation that is counterbalanced by a simultaneous decrease in the number of islands due to coalescence. Depending on temperature, the saturation occurs in our simulations after one second or more, corresponding to deposition of about 0.1 ML (see Fig. 3).

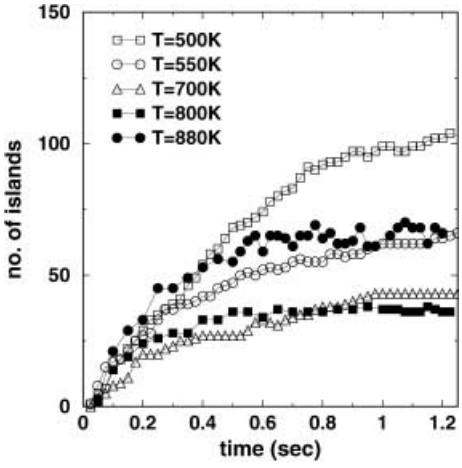

Fig. 3. Time evolution of the island densities in the new layer in a simulation area of 160×320 surface lattice constants at various temperatures for a Ga flux of 0.1 ML/s and an As_2 pressure of 8.5×10^{-7} bar

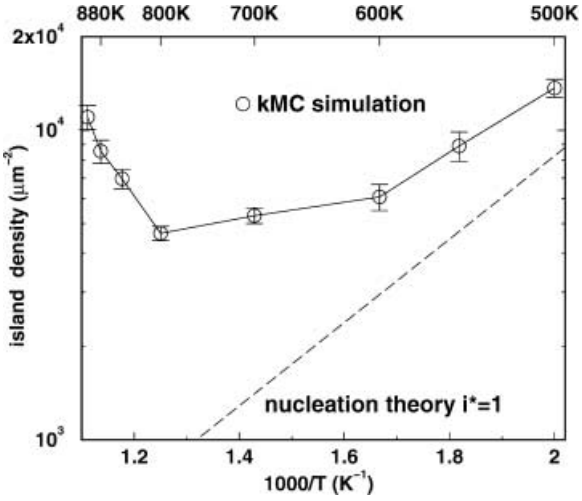

Fig. 4. Saturation island density as a function of the inverse growth temperature. The *dashed line* shows the prediction of nucleation theory for diffusion-limited attachment and a critical nucleus size equal to 1, using the Ga diffusivity along [110], $D = D_0 \exp(-0.8\,\mathrm{eV}/k_\mathrm{B}T)$. The fluxes of Ga and As_2 are the same as in Fig. 3

We note that some caution is needed when relating the temperature scale in the simulations to measured temperatures. While DFT calculations can reliably predict the relative sequence of barrier heights, absolute barrier heights are not available yet with an accuracy better than ± 0.1 eV. A 10% error in all barriers, for instance, would shift the temperature scale by the same relative amount. Because of this uncertainty, we decided to perform simulations over a wide temperature range, from 500 K up to 900 K. In addition, systematic studies of the island density as a function of substrate temperature are of interest because they have been widely used to derive the diffusion constant for adatoms as well as its temperature dependence from measurements of the island density [50–53]. The extraction of the diffusion constant from the experimental data is made under the assumption that nucleation theory is valid in its variant describing diffusion-limited attachment. In this case, the island density is a monotonically decreasing function of the growth temperature.

In order to check whether island nucleation on GaAs can be described by this frequently used theory, results from a systematic study of the island density as a function of growth temperature are displayed in Fig. 4. We find a decrease of the saturation island density when the substrate temperature is increased from 500 K to 600 K. This behavior is consistent with nucleation theory, if one assumes diffusion-limited nucleation of islands with a critical nucleus size $i^* = 1$. However, in the simulations the island density comes out to be almost constant above 600 K, and even increases again for $T > 800$ K. The reason for this unusual non-monotonic behavior becomes clear when one considers the balance of material flow for As at the growing surface shown in Fig. 2. At low temperatures and sufficiently high As_2 partial pressures, supply is dominated by $F^{(3)}_{\mathrm{ads}}$, i.e. by the complexes of three $\mathrm{Ga} + \mathrm{As}_2$. At higher temperature, the initially formed Ga–As–As–Ga_2 complexes become unstable against As_2 desorption. A decreasing fraction of them can stabilize by capturing a Ga adatom and forming a more long-lived Ga_2–As–As–Ga_2 complex. Due to the decay of the Ga–As–As–Ga_2 intermediate at high temperatures, island edges are effectively less 'sticky' for diffusing Ga adatoms than at low temperatures. This, in turn, leads to a higher density of mobile Ga adatoms, a higher nucleation rate of new islands, and thus to the observed rise of the saturation island density at temperatures above 800 K.

Additional information can be obtained from inspecting how the island morphology evolves during the simulations. Figure 5a shows that growth below $T = 700$ K proceeds mainly by trench-filling. At higher temperatures, an increasing fraction of islands also extends into the regions in between trenches, forming a new layer of material. The increasing amount of material grown in this new layer is related to the reversibility of As_2 adsorption and desorption from Ga–As–As–Ga_2 complexes at temperatures above $T = 800$ K. As a consequence, structures grown in the trenches can dissolve again, and the material remobilized in this way gets attached to islands that extend into the new layer. The influence of growth temperature becomes apparent by comparing the island morphology at $T = 700$ K in Fig. 5a and $T = 900$ K in Fig. 5b. In Fig. 5a most of the deposited material fills in the trenches of the $\beta 2$ reconstructions (grey vertical columns), while a smaller fraction appears in the new layer. In Fig. 5b, we see filled trenches only if they are part of islands that extend into the new layer. The latter is consistent with STM images recorded after growth of ~ 0.1 ML [54].

The simulated island densities agree with those obtained from STM experiments. Experimentally, the island density increases with higher V/III ratio, from 3400 to 6600 $\mu\mathrm{m}^{-2}$ [54, 55] for growth with an As_2 beam. The simulations yield an island density of 4600 $\mu\mathrm{m}^{-2}$ in the temperature range between $T = 700$ K and 800 K, where the temperature dependence is weak. Reducing the As_2 flux by an order of magnitude at 700 K in the simulations resulted in a decrease of the island density, in accordance with the experimental findings.

Measurements of the island density after sub-monolayer deposition have been used to derive an experimental estimate of the diffusivity of adatoms [51–53]. In the data analysis, it is usually assumed that the island density is described by nucleation theory in its particular form applicable to diffusion-

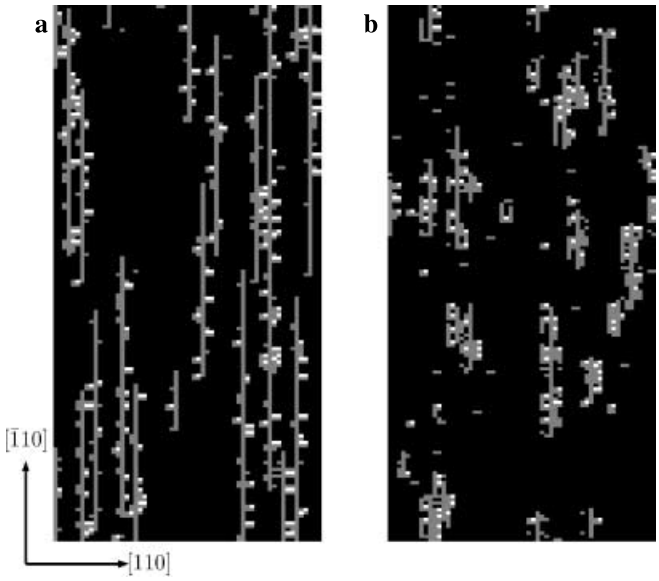

Fig. 5a,b. Surface morphology shown on a scale of 80×160 lattice sites after growth of 0.1-ML GaAs at $T = 700$ K (**a**) and $T = 900$ K (**b**). Islands are shown in *grey*, As dimers deposited in the new layer in *white*

limited nucleation with a critical nucleus $i^* = 1$. In this case, the island density as a function of temperature T is predicted to increase like $(F/D(T))^{1/3}$, where F is the flux of Ga atoms and $D(T)$ is the diffusivity. We note that the island density at typical growth temperatures both in experiment and in our simulations is an order of magnitude higher than predicted by these conventional arguments. In contrast to this prediction, but in agreement with our simulations, a homoepitaxial film of GaAs evolves by coalescence of an unusually large number of small islands elongated along the $[\bar{1}10]$ direction. Our investigation thus demonstrates that some caution is in order when deriving information about diffusivities from measured island densities. Given the rather complex $\beta 2(2 \times 4)$ reconstruction of the GaAs (001) surface, one would expect that coalescence of islands gives rise to disorder in the film when two islands whose (2×4) unit meshes are not aligned start to touch each other. In order to achieve good film quality, it is therefore desirable to keep the nucleation density of islands as low as possible. Our simulations indicate a minimum of the island density at a growth temperature of about 800 K, where desorption of As_2 starts to become relevant on the time scale of deposition. The temperature window frequently used by MBE crystal growers is a compromise between the Ga adatom mobility and the lifetime of As_2–Ga complexes that yields the lowest possible island density.

Summarizing the section about homoepitaxy of GaAs, we stress that our main goal is an understanding of the consequences of DFT results for the growth kinetics of GaAs at various temperatures. In contrast, the atomistic growth model of Itoh et al. ([14], for a detailed description of this model see [16]) is based on parameters that are obtained by adjusting experimental and simulated island morphologies at a single growth temperature, 873 K. The information available from the DFT calculations motivated us to include several features in our simulations that were not considered previously: most importantly, the incorporation of As_2 via an intermediate state where the arsenic molecule forms three bonds to the surface (rather than four) has not been considered before. Moreover, we include a detailed description of the Ga diffusion processes in our modeling. In our simulations, formation of new structures is possible by agglomeration of Ga atoms and As_2 molecules both in the trenches and in the new layer; and the growth conditions decide about the relative importance of these two possibilities. This is in contrast to earlier simulations guided by experimental results [14], which took the experimentally observed island morphologies as evidence for a nucleation process starting exclusively in the new layer.

2 Heteroepitaxy of InAs on GaAs

From the technological point of view, epitaxial growth is of considerable importance because it has made it possible to grow semiconductor heterostructures in a controlled way. For instance, heterostructures of III–V compounds have been used to achieve planar confinement of charge carriers in quantum wells and to realize a two-dimensional electron gas with high carrier mobility. In recent years, the heteroepitaxial growth of InAs on GaAs has received much attention in the context of fabrication of quantum dots. By depositing a few monolayers of InAs on GaAs (001), spontaneous evolution of nanometer-sized islands (so-called self-assembly) was observed. After growing a capping layer of GaAs on top the nanostructured film, the buried islands, consisting mainly of InAs, can be used for confinement of charge carriers in all three spatial dimensions, due to the lower band gap of InAs compared to the surrounding GaAs matrix. Under judiciously chosen experimental conditions, the deposited material forms elastically strained, defect-free three-dimensional islands (for a review, see e.g. [56]). After overgrowth with a capping layer of suitable material, and possibly after repeating the procedure of islanding and overgrowth several times, the resulting quantum-dot (QD) structures lend themselves to a variety of applications, foremost in optoelectronic devices such as light-emitting diodes and quantum-dot lasers [57]. The latter have been based on stacked layers of QDs separated by thin smooth capping layers. For the use of these nanostructures in laser devices, it is crucial that the islands resulting from the growth process are homogeneous in size, because a spread in the size distribution would result in non-resonant optical transitions in the individual QDs, and thus spoil the basic operating mechanism of the laser.

To a first approximation, the self-assembly of islands can be understood as a form of growth in the Stranski–Krastanow regime. According to this point of view, based on thermodynamic arguments, the deposited material starts to grow as a homogeneous wetting layer, because it has a lower surface energy than the substrate. Only after a critical thickness of this layer has been exceeded, does the growth of three-dimensional islands that allow for partial elastic strain relaxation become energetically preferable to the two-dimensional film growth. These three-dimensional islands, once nucleated, start to grow at the expense of the wetting layer, thereby competing for the available material, until they have reached an optimum size [58, 59]. This description of three-dimensional island growth is rather general since it employs mainly thermodynamic arguments. Kinetics enters in this theory only as an external parameter, the island density, that is determined during the nucleation phase and assumed to remain constant during three-dimensional growth of the

islands. A more detailed picture of the formation process should not only account for nucleation kinetics, but also for the kinetic aspects of growth. While the stochastic nature of the nucleation process is expected to give rise to some irregularities in the spatial arrangement as well as to a broad size distribution of the islands, it has been demonstrated experimentally that the heteroepitaxial self-assembly process leads to more regular structures, sometimes with a narrow size distribution. In particular, improved homogeneity is found in stacked QD systems when going from the seed layer to higher and higher layers in the stack. Since these features are essential for the usefulness of the self-assembled nanostructures as quantum dots and for their envisaged application in future electronic devices, it is tempting to speculate that they constitute intrinsic features of the growth process. Various mechanisms that could lead to narrow size distributions have been suggested in the literature [58–63].

Here, we shall discuss the role of strain for the evolution of islands. Each coherently strained island introduces a strain field around it in the substrate, leading to lateral elastic interaction between uncovered islands when a single sheet of quantum dots is grown. In addition, in multi-sheet arrays of quantum dots, strain gives rise to interactions between islands in different sheets separated by the capping layer. We will come back to this issue later.

For uncovered islands in a single sheet, earlier studies in the literature have found that the direct elastic interaction of islands becomes important only at rather high island densities, when the distance between islands is comparable to their base length [64, 65].

However, in addition to this direct interaction, strain also affects the adatom density on the substrate surface during growth. For adatoms that are locally in equilibrium with a wetting layer on the substrate, a thermodynamic treatment within a mechanical continuum model, introducing a spatially varying chemical potential for the adatoms, has been proposed (see e.g. [66, 67]). Yet, little is known about the effect of strain on the kinetics of growth due to changes of the diffusivity of adatoms that governs the material transport on the substrate surface towards an evolving island.

Here, we shall report recent DFT calculations to investigate this aspect for a particular example, the adsorption and surface diffusion of indium during heteroepitaxy of InAs on GaAs (001). This system is characterized by a lattice mismatch $(a_{\mathrm{InAs}} - a_{\mathrm{GaAs}})/a_{\mathrm{GaAs}} = \Delta a/a = 7.2\%$. To be specific, we study In adatom diffusion on the $c(4\times4)$-reconstructed GaAs (001) surface that is experimentally observed in the initial stages of InAs deposition in the low-temperature growth regime, $T < 500\,^{\circ}\mathrm{C}$ [30]. The geometric structure of this surface is described as follows: on top of a complete As surface layer, the $c(4\times4)$ reconstruction has rows of As dimers running in the $[\bar{1}10]$ direction, with units of three As dimers interrupted by a dimer vacancy. The geometric structure of the surface, together with the PES for In diffusion obtained from DFT calculations, is shown in Fig. 6. The calculations show that it is the dimer vacancy site $\boldsymbol{A}_1$ where a deposited In atom is adsorbed most strongly. Diffusion is dominated by hopping through the transition state $\boldsymbol{T}_1$. From an analysis of the PES we conclude that diffusion is activated by 0.65 eV and slightly anisotropic.

Since the elastic distortions in the vicinity of strained heteroepitaxial islands vary slowly on the atomic scale, we

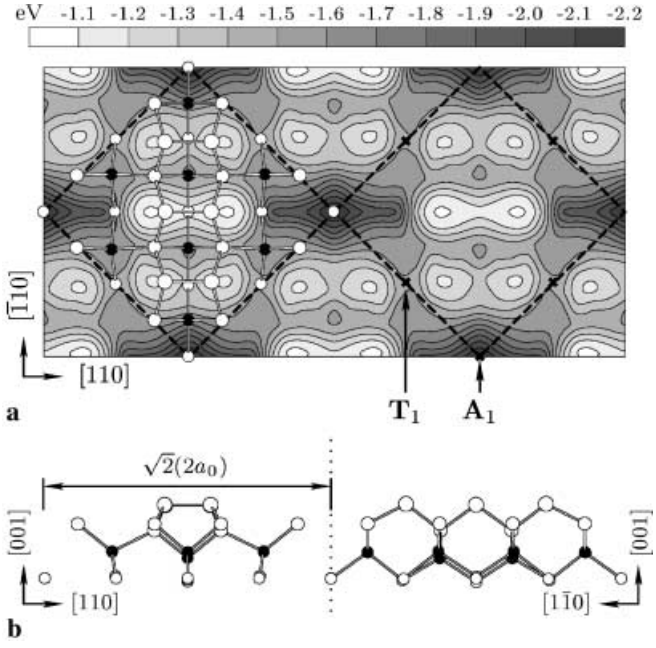

Fig. 6. a Potential-energy surface for an In adatom on the GaAs (001)-$c(4\times4)$ surface. The positions of the atoms in the four topmost layers in the clean surface unit cell are indicated (As: *empty circles*; Ga: *filled circles*). The *dashed boxes* indicate the surface unit cell. *Side views* are shown in **b**

can study the effect of strain, ε, within the first-principles approach by performing DFT calculations for uniformly strained slabs that mimic the local strain state $\varepsilon(\boldsymbol{r}_\parallel)$ of the substrate surface, $\boldsymbol{r}_\parallel$ being a coordinate parallel to the surface. In particular, we investigate the strain dependence of the In binding energy, $E_{\mathrm{b}}(\varepsilon)$. This quantity is crucial for the lateral variation of the In concentration on the surface when a stationary average In coverage is maintained by an equilibrium between supply from an atomic In beam and loss due to evaporation of In. In this case, the adatom density is given by

$$n(\boldsymbol{r}_\parallel) = n_0 \exp[E_{\mathrm{b}}(\varepsilon(\boldsymbol{r}_\parallel))/k_{_B}T]\,. \tag{1}$$

Since the nucleation probability is an increasing function of the adatom density n, the surface regions with enhanced adatom binding due to strain will show an enhanced probability of island nucleation. The described effect of strain is most pertinent to QD stacks: the vertical correlation of quantum dots in adjacent layers is controlled by the nucleation of the first islands on the capping layer. The strain fields of buried islands in deeper layers affect the adatom density and thus the nucleation probability on the capping layer. For a single buried InAs island in a GaAs capping layer, calculations using continuum elasticity theory have shown that the surface lattice of the capping layer is expanded in the region above the island [68]. In addition, our DFT calculations demonstrate that the binding of In adatoms is enhanced for positive (tensile) strain and decreased for negative (compressive) strain. The effect can be described approximately by a linear strain dependence of the binding energy,

$$E_{\mathrm{b}}(\varepsilon) = 2.2\,\mathrm{eV} + \varepsilon \times 3.8\,\mathrm{eV}\,. \tag{2}$$

The linear variation of the binding energy with strain can be rephrased in terms of a change of the surface stress induced

by the adsorbate. Apart from the linear effect, the calculated data also show a non-linear contribution to the strain dependence of binding energies.

Given the elastic expansion of the capping layer above a buried island, combining (1) and (2) puts us in a position to conclude that the growth of QD stacks in the InAs/GaAs materials system is characterized by preferred nucleation of new InAs islands above the largest buried islands in the layer below. This result explains the observed correlation of InAs dots between subsequent layers in the GaAs matrix. Furthermore, it has been pointed out that the dominance of large islands acting as a seed for the nucleation in the new layer gradually improves the regularity of the in-plane orientation of quantum dots as well as their size homogeneity [69].

Another possibility how strain could affect the kinetics of island growth is by changing the mobility of adatoms diffusing on the surface. During the growth process, the growing islands compete for the deposited material. A self-limiting growth mechanism is conceivable that leads to a narrow island size distribution, provided that the flow of material towards the largest islands is hindered by their surrounding strain field. For materials systems of interest for quantum dots, such as Ge/Si and InAs/GaAs, the free-standing heteroepitaxial islands are under compressive strain at their base, while the substrate beneath the island is expanded. As a consequence of this expansion, the substrate surface around an island is under compressive strain (see e.g. Fig. 2 in [70]).

For islands on the $c(4\times4)$-reconstructed GaAs surface, (2) implies that the binding of a diffusing In adatom is reduced for sites close to the island. In other words, the island gives rise to a repulsive potential that raises the bottom of the well of the migration potential of an adatom. We have also investigated the strain dependence of the energy of the transition state $\boldsymbol{T}_1$ with the help of DFT calculations. For diffusion near the island, the transition states are also raised in energy, albeit not by exactly the same amount as the binding state.

In summary, our calculations show, for the particular case of coherently strained InAs islands surrounded by the $c(4\times4)$-reconstructed GaAs surface, that the strain field around an island will hinder the diffusive flow of material towards the island and thus have a self-limiting effect on island growth. In most experimental situations, the InAs islands grow in the presence of a wetting layer on the GaAs substrate. The effect of strain on the diffusion on top of a wetting layer is subject to ongoing research.

A scenario can be worked out explicitly for a simple geometry, a very elongated, shallow island that is coherently strained (Fig. 7). Within the framework of continuum elasticity theory, the strained island gives rise to a change of the stress component parallel to the surface across the island edge, denoted by $\Delta\sigma$. The resulting force monopole generates a strain field in front the island that can be calculated analytically within linear elasticity theory (see [71] and references therein). If x measures the distance for perpendicular approach to a quasi-one-dimensional island with its edge at $x=0$, the strain field has the form

$$\varepsilon(x) = \eta\,\Delta\sigma\,\tan\theta\,\ln\left|\frac{P_2(x)}{Q_2(x)}\right| . \qquad (3)$$

The island geometry (height h, base length s, and the tilt angle of the side facets θ) determines the coefficients in the second-order polynomials $P_2(x)$ and $Q_2(x)$, whereas the elastic properties of the materials system enter the prefactor η. An explicit calculation for an elastically isotropic substrate yields $P_2(x) = (h\cot\theta + x)(s - h\cot\theta + x)$, $Q_2(x) = x(s+x)$. The prefactor is given by $\eta = 2(1+\nu)(1-\nu)/(\pi Y)$, where ν is the Poisson ratio and Y is Young's modulus of the substrate. Neglecting the effect of elastic relaxation of the island, the magnitude of $\Delta\sigma$ is estimated to be $\Delta\sigma \approx Y\Delta a/a$, i.e. it is proportional to the lattice mismatch $\Delta a/a$ between the island and the substrate. By combining the DFT result expressed in (2) with the knowledge of the long-range strain field obtained from linear elasticity theory, we can assess the effect of strain on the transport of deposited material towards an island. Figure 7 illustrates a result for a particular geometry obtained by substituting $\varepsilon(x)$ from (3) into (2), for an InAs island on GaAs with height $h = 2$ nm and base length $s = 16$ nm. As can be seen from the figure, the effect of strain leads to a repulsive potential with a strength of up to 0.2 eV, that affects both the binding energy and, to a slightly smaller extent, the diffusion barriers for an In adatom that attempts to approach this island. This repulsive interaction can significantly slow down the speed of growth of strained islands. It is worthwhile to perform further investigations of the growth kinetics to study its effect in detail.

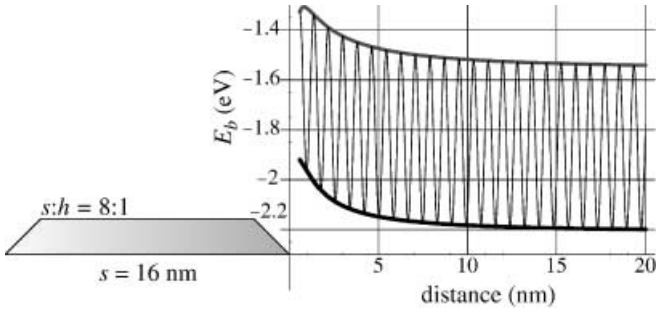

Fig. 7. Migration potential (oscillating curve) for an In adatom approaching perpendicularly to a very long, coherently strained InAs island on the $c(4\times4)$-reconstructed GaAs (001) surface. In addition to the diffusion potential due to the atomic structure of the surface, the strain field in the substrate induced by the island gives rise to a repulsive potential that lifts both the binding energies (*thick lower line*) and transition-state energies (*thick upper line*) close to the island

Thus our investigations provide an example for a materials system (In diffusion on strained GaAs (001)-$c(4\times4)$) with the unusual property that smaller islands grow faster than larger islands: since the strain field around an island becomes stronger with increasing island size, the effect of strain leads to retarded growth of larger islands, and gives the smaller islands the chance to catch up during growth. For a simple example, where two very elongated islands compete for the flux of In atoms deposited between them, we find that strain-controlled diffusion indeed tends to equalize the size of the two islands while they are growing [72]. This effect has been proposed as one of the factors responsible for the narrowing of the island-size distribution that is desirable from the point of view of the applications [73, 74].

3 Conclusion

We have presented investigations of the kinetic aspects of epitaxy using a combination of methods from statistical me-

chanics and electronic-structure theory in order to treat phenomena at surfaces such as adsorption, diffusion, and island nucleation and growth. The density-functional calculations used to obtain the energetics of these processes constitute a parameter-free approach that enables us to make predictions independent from experimental input. Following this approach, computational modeling has evolved into an independent research tool complementary to experiments, whose outcome can and should be tested against experimental data. The use of multi-scale modeling techniques, such as the combination of electronic-structure calculations with kinetic Monte Carlo simulations of kinetics, makes it possible to retain the attractive features of first-principles calculations, while enabling us at the same time to address problems in physics or chemistry of surfaces on the experimentally relevant length and time scales. The combination of experimental research and theoretical concepts developed from computer simulations eventually results in an improved understanding of the processes behind epitaxial growth on the atomic level. Moreover, computational physics enables us to address subtle aspects of the kinetics of growth that are hard to probe directly in an experiment, but can have important consequences for the growth morphology. As an example, we have discussed the role of strain for the material transport in heteroepitaxial systems.

Acknowledgements. We would like to acknowledge fruitful discussions with F. Grosse, M. Itoh, T. Mishonov, C.M. Morgan, and D.D. Vvedensky. This work was supported by the Deutsche Forschungsgemeinschaft, Sfb 296.

References

1. A. Groß, M. Scheffler: Prog. Surf. Sci. **53**, 187 (1998)
2. G.-J. Kroes: Prog. Surf. Sci. **60**, 1 (1999)
3. C.T. Foxon, B.A. Joyce: Surf. Sci. **64**, 293 (1977)
4. S.V. Ghaisas, A. Madhukar: Phys. Rev. Lett. **56**, 1066 (1986)
5. S.V. Ghaisas, A. Madhukar: SPIE Proc. **944**, 16 (1988)
6. T. Shitara, D.D. Vvedensky, M.R. Wilby, J. Zhang, J.H. Neave, B.A. Joyce: Phys. Rev. B **46**, 6815 (1992)
7. P. Smilauer, M.R. Wilby, D.D. Vvedensky: Phys. Rev. B **47**, 4119 (1993)
8. F. Grosse, R. Zimmermann: J. Cryst. Growth **212**, 128 (2000)
9. C. Heyn, M. Harsdorff: Phys. Rev. B **55**, 7034 (1997)
10. C. Heyn, M. Harsdorff: Phys. Rev. B **56**, 13 483 (1997)
11. C. Heyn, T. Franke, R. Anton: J. Cryst. Growth **201–202**, 67 (1999)
12. A. Ishii, T. Kawamura: Appl. Surf. Sci. **130–132**, 403 (1998)
13. A. Ishii, T. Kawamura: Surf. Sci. **436**, 38 (1999)
14. M. Itoh, G.R. Bell, A.R. Avery, T.S. Jones, B.A. Joyce, D.D. Vvedensky: Phys. Rev. Lett. **81**, 633 (1998)
15. M. Itoh, G.R. Bell, B.A. Joyce, D.D. Vvedensky: Prog. Theor. Phys. Suppl. **138**, 90 (2000)
16. M. Itoh: Prog. Surf. Sci. **66**, 53 (2001)
17. P. Ruggerone, C. Ratsch, M. Scheffler: in *The Chemical Physics of Solid Surfaces*, Vol. 8, ed. by D.A. King, D.P. Woodruff (Elsevier, Amsterdam 1997) pp. 490–544
18. A. Bogicevic, J. Strömquist, B.I. Lundqvist: Phys. Rev. Lett. **81**, 637 (1998)
19. S. Ovesson, A. Bogicevic, B.I. Lundqvist: Phys. Rev. Lett. **83**, 2608 (1999)
20. K.A. Fichthorn, M. Scheffler: Phys. Rev. Lett. **84**, 5371 (2000)
21. D.J. Chadi: J. Vac. Sci. Technol. A **5**, 834 (1987)
22. G. Qian, R.M. Martin, D.J. Chadi: Phys. Rev. B **38**, 7649 (1988)
23. J.E. Northrup, S. Froyen: Phys. Rev. Lett. **71**, 227 (1993)
24. J.E. Northrup, S. Froyen: Phys. Rev. B **50**, 2015 (1994)
25. N. Moll, A. Kley, E. Pehlke, M. Scheffler: Phys. Rev. B **54**, 8844 (1996) [cond-mat/9607005]
26. W.G. Schmidt, S. Mirbt, F. Bechstedt: Phys. Rev. B **62**, 8087 (2000)
27. V.P. LaBella, H. Yang, D.W. Bullock, P.M. Thibado, P. Kratzer, M. Scheffler: Phys. Rev. Lett. **83**, 2989 (1999)
28. C. Ratsch, W. Barvosa-Carter, F. Grosse, J.H. Owen, J.J. Zinck: Phys. Rev. B **62**, R7719 (2000)
29. R.H. Miwa, G.P. Srivastava: Phys. Rev. B **62**, 15 778 (2000)
30. B.A. Joyce, D.D. Vvedensky, A.R. Avery, J.G. Belk, H.T. Dobbs, T.S. Jones: Appl. Surf. Sci. **132**, 357 (1998)
31. D.K. Biegelsen, R.D. Bringans, J.E. Northrup, L.-E. Schwartz: Phys. Rev. B **41**, 5701 (1990)
32. S.-H. Lee, W. Moritz, M. Scheffler: Phys. Rev. Lett. **85**, 3890 (2000)
33. C. Kumpf, L.D. Marks, D. Ellis, D. Smilgies, E. Landemark, M. Nielsen, R. Feidenhans'l, J. Zegenhagen, O. Bunk, J.H. Zeysing, Y. Su, R.L. Johnson: Phys. Rev. Lett **86**, 3586 (2001)
34. E.S. Tok, J.H. Neave, J. Zhang, B.A. Joyce, T.S. Jones: Surf. Sci. **374**, 397 (1997)
35. P. Kratzer, C.G. Morgan, M. Scheffler: Phys. Rev. B **59**, 15 246 (1999) [cond-mat/9905118]
36. C.G. Morgan, P. Kratzer, M. Scheffler: Phys. Rev. Lett. **82**, 4886 (1999)
37. P. Kratzer, C.G. Morgan, M. Scheffler: Prog. Surf. Sci. **59**, 135 (1998)
38. C.G. Morgan, P. Kratzer, M. Scheffler: to be published
39. K. Shiraishi: Thin Solid Films **272**, 345 (1996)
40. A. Kley, P. Ruggerone, M. Scheffler: Phys. Rev. Lett. **79**, 5278 (1997)
41. J.G. LePage, M. Alouani, D.L. Dorsey, J.W. Wilkins, P.E. Blöchl: Phys. Rev. B **58**, 1499 (1998)
42. K. Seino, A. Ishii, T. Aisaka: Surf. Sci. **438**, 43 (1999)
43. C. Ratsch, A. Seitsonen, M. Scheffler: Phys. Rev. B **55**, 6750 (1997)
44. A. Kley: *Theoretische Untersuchungen zur Atomdiffusion auf niedrigindizierten Oberflächen von* GaAs (Wissenschaft & Technik, Berlin 1997)
45. K. Shiraishi, T. Ito: Phys. Rev. B **57**, 6301 (1998)
46. B.A. Banse, J.R. Creighton: Appl. Phys. Lett. **60**, 856 (1992)
47. T. Ito, K. Shiraishi: Surf. Sci. **357–358**, 486 (1996)
48. T. Ito, K. Shiraishi: Surf. Sci. **386**, 241 (1997)
49. M. Pristovsek, T. Trepk, M. Klein, J. Zettler, W. Richter: J. Appl. Phys. **87**, 1245 (2000)
50. H. Brune: Surf. Sci. Rep. **31**, 121 (1998)
51. Y.-W. Mo, J. Kleiner, M.B. Webb, M.G. Lagally: Phys. Rev. Lett. **66**, 1998 (1991)
52. Y.-W. Mo, J. Kleiner, M.B. Webb, M.G. Lagally: Surf. Sci. **268**, 275 (1992)
53. V.P. LaBella, D.W. Bullock, Z. Ding, C. Emery, W.G. Harter, P.M. Thibado: J. Vac. Sci. Technol. A **18**, 1526 (2000)
54. G.R. Bell, M. Itoh, T.S. Jones, B.A. Joyce: Surf. Sci. **423**, L280 (1999)
55. B.A. Joyce, D.D. Vvedensky, T.S. Jones, M. Itoh, G.R. Bell, J.G. Belk: J. Cryst. Growth **201–202**, 106 (1999)
56. V.A. Shchukin, D. Bimberg: Rev. Mod. Phys. **71**, 1125 (1999)
57. N. Kirstaedter, N.N. Ledentsov, M. Grundmann, D. Bimberg, V.M. Ustinov, S.S. Ruvimov, M.V. Maximov, P.S. Kop'ev, Z.I. Alferov, U. Richter, P. Werner, U. Gösele, J. Heydenreich: Electron. Lett. **30**, 1416 (1994)
58. L.G. Wang, P. Kratzer, M. Scheffler, N. Moll: Phys. Rev. Lett. **82**, 4042 (1999) [cond-mat/9905122]
59. L.G. Wang, P. Kratzer, N. Moll, M. Scheffler: Phys. Rev. B **62**, 1897 (2000)
60. V.A. Shchukin, N.N. Ledentsov, P.S. Kop'ev, D. Bimberg: Phys. Rev. Lett. **75**, 2968 (1995)
61. C. Priester, M. Lannoo: Phys. Rev. Lett. **75**, 93 (1995)
62. Y. Chen, J. Washburn: Phys. Rev. Lett. **77**, 4046 (1996)
63. D.E. Jesson, G. Chen, K.M. Chen, S.J. Pennycook: Phys. Rev. Lett. **80**, 5156 (1998)
64. V.A. Shchukin, D. Bimberg: Appl. Phys. A **67**, 687 (1998)
65. A. Ponchet, D. Lacombe, L. Durand, D. Alquier, J.M. Cardonna: Appl. Phys. Lett. **72**, 2984 (1998)
66. D.J. Srolovitz: Acta Metall. **37**, 621 (1989)
67. Q. Xie, A. Madhukar, P. Chen, N.P. Kobayashi: Phys. Rev. Lett. **75**, 2542 (1995)
68. V. Holý, G. Springholz, M. Pinczolits, G. Bauer: Phys. Rev. Lett. **83**, 356 (1999)
69. J. Tersoff, C. Teichert, M.G. Lagally: Phys. Rev. Lett. **76**, 1675 (1996)
70. N. Moll, M. Scheffler, E. Pehlke: Phys. Rev. B **58**, 4566 (1998) [cond-mat/9807200]
71. J. Tersoff, R.M. Tromp: Phys. Rev. Lett. **70**, 2782 (1993)
72. E. Penev, P. Kratzer, M. Scheffler: Phys. Rev. B **64**, 085401 (2001) [cond-mat/0105397]
73. A. Madhukar: J. Cryst. Growth **163**, 149 (1996)
74. H.M. Kudovely, A. Zangwill: Phys. Rev. B **60**, R2204 (1999)